MCBI in an Electron-Ion Collider*

R. Li

Thomas Jefferson National Accelerator Facility, Newport News, VA 23693, USA

Abstract

The luminosity performance for an electron-ion collider demands high-current operation for both the electron and ion beams, for a wide range of collision energies. This poses many challenges on the beam stability with regard to collective effects. In this paper, we present preliminary estimations of coherent instabilities for both of the EIC designs, i.e., JLEIC and eRHIC. Mitigation mechanisms or schemes envisioned for suppression of the instabilities are also discussed.

INTRODUCTION

An electron-ion collider (EIC) is identified by the nuclear physics community as the next exploring machine for answering fundamental questions about QCD structure and dynamics of nuclear matter. To serve this goal, such collider needs to have a wide range of centre-of-mass energy (20-140 GeV), high luminosity (10^{33} ~10^{34} cm^{-2} sec^{-1}), a wide range of ion species, and high polarization (~70%) for the electron and light ion beams. In the past two decades, two EIC designs were actively developed, i.e., eRHIC by BNL and JLEIC by Jefferson Lab. Recently after BNL was selected to host EIC, the two labs joined forces in bringing eRHIC to the ultimate EIC.

The luminosity performance of an EIC requires stable beam operation, while the behaviour of beam instability is determined by the luminosity concepts of the collider design. Despite the differences in machine configuration and in detailed parameters, JLEIC and eRHIC share similar luminosity concepts that resemble those used in lepton colliders [1]. For both designs, the high luminosity is achieved by high beam current operation with moderate bunch charge, small transverse bunch emittances, small vertical beta star and a high bunch repetition rate. Here the small beta star is enabled by short bunch length, which is a new regime for hadron beams. The high rep rate is enabled by crab cavities to prevent parasitic collisions. At highest luminosity, a high-energy bunched electron cooling is applied to the hadron beam, making the small transverse emittance and energy spread possible. These features of bunch distribution pattern, i.e., moderate bunch charge, small transverse emittances, and high bunch rep rate, imply that the beams at low energy could be vulnerable to single and coupled bunch instabilities, as well as two-stream instabilities. For a complete design study, the collective effects need to be assessed for a wide range of beam energies and ion species, and also for the entire ion bunch formation process. In this paper, we present preliminary estimations of coherent instabilities for JLEIC, for cases of a few selected collision energies, and discuss possible mitigation schemes. The counterpart studies for eRHIC will also be highlighted.

* This material is based upon work supported by the U.S. Department of Energy, Office of Science, Office of Nuclear Physics under contract DE-AC05-06OR23177.

MCBI IN JLEIC

The layout of JLEIC is shown in Fig. 1. In this design, the existing CEBAF is used as the full-energy electron beam injector, and the figure-8 shape is chosen for the collider rings to optimize polarization preservation. Table 1 shows the key parameters relevant to the collective effects for the JLEIC [2], and parameters of PEPII are listed for comparison. In the following, we discuss the beam stability at the collision scenarios for the electron beam at energies E_e=3, 5, 10 GeV and for the proton beam at E_p=100 GeV.

The back-of-envelop assessments are given for impedance-driven instabilities, i.e., single and coupled bunch instabilities, as well as for two-stream instabilities, i.e., the e-cloud effects in the ion ring and the ion effects in the electron ring. This exercise helps us to identify parameter regimes vulnerable to beam instabilities where additional studies and mitigation schemes are called for.

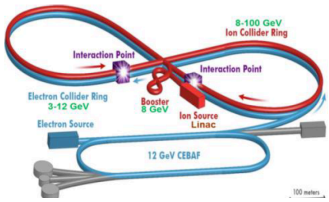

Figure 1: Schematic layout of JLEIC

Table 1: Parameters for JLEIC Instability Estimation

	PEP-II (LER)	**JLEIC** e-Ring			**JLEIC** p-Ring
E [GeV]	3.1	3	5	10	100
I_{ave} [A]		2.8	2.8	0.71	0.98
I_p [A]	113	59.0	59.0	50.6	15.6
η (10^{-3})	1.31	1.09			6.22
σ_δ (10^{-4})	7.7	2.78	4.64	9.28	3.0
υ_s (10^{-2})	3.7	0.88	1.46	2.51	5.3
$\langle\beta_\perp\rangle$ [m]	20	13			18

Impedance Budget

The budget of machine broadband impedance requires detailed engineering drawings and careful EM modelling. For initial estimations, we start with the component counts for JLEIC collider rings and use impedance budgets in existing machines, such as PEPII or SUPERKEKB, as references [3, 4, 5]. One reason for using PEPII for reference is that there is consideration for the JLEIC e-ring to adopt the RF cavities, as well as the components for the vacuum and diagnostic systems, from PEPII HER. Another convenient feature is that the bunch length ($\sigma_z \approx 1.2$ cm) for JLEIC is comparable to that in PEPII, given that the effective impedances are bunch-length dependent. With the PEPII impedance budget and the JLEIC component counts, and assuming these components are identical with those used in the PEPII HER, we get the estimation for the JLEIC e-ring: the inductance $L \approx 99.2$ nH, the effective longitudinal impedance $\left|Z_{\parallel}/n\right| \approx 0.09\ \Omega$, the loss factor $k_{\parallel} \approx 7.7$ V/pC, and the effective transverse impedance $\left|Z_{\perp}\right| \approx 60$ kΩ/m. If components in SUPERKEKB are used as reference, the JLEIC e-ring impedance estimation becomes:

$L \approx 28.6$ nH, $\left|Z_{\parallel}/n\right| \approx 0.02\Omega$, $k_{\parallel} \approx 19$ V/pC, $\left|Z_{\perp}\right| \approx 13$ kΩ/m,

with the note that a shorter bunch length ($\sigma_z \approx 0.5$ cm) for beams in SUPERKEKB than that in JLEIC may cause underestimation of the effective impedances.

For the JLEIC ion ring, the ion beam undergoes the bunch formation process including the injection, acceleration, bunch splitting, and finally collision. The bunch length varies through the whole process, and the short ion bunch ($\sigma_z \approx 1.2$ cm) at the collision stage is made possible only by employing the envisioned high-energy electron cooling [6]. Since such short bunch length is unprecedented for the ion beams in existing ion rings, it is more appropriate [7] to use the PEPII rings (rather than existing ion rings) for reference when we estimate the impedance budget for the JLEIC ion ring. The ion-ring impedance at the collision scenario is thus estimated as:

$L \approx 97.6$ nH, $\left|Z_{\parallel}/n\right| \approx 0.08\ \Omega$, $k_{\parallel} \approx 8.6$ V/pC, $\left|Z_{\perp}\right| \approx 80$ kΩ/m.

Note that some special components unique to the JLEIC design, such as the crab cavities and IR chamber, require detailed impedance modelling because references from the existing machines are either inadequate or not available.

Longitudinal Microwave Instability (LMWI)

The LMWI is assessed here by comparison between the theoretical estimation of impedance threshold, as given by the Keil-Schnell criterion,

$$\left|\frac{Z_{\parallel}(n)}{n}\right|^{\text{th}} \approx \frac{2\pi\beta^2\left|\eta\right|E\sigma_{\delta}^2}{eI_{\text{peak}}},$$

and the expected machine impedance $\left|Z_{\parallel}/n\right|^{\text{ring}}$. For the JLEIC baseline parameters in Table 1, this comparison is shown in Table 2, where "s", "u", and "m" denote stable, unstable and marginal respectively. Note that for the JLEIC electron beam, the energy spread gets smaller at lower energies. As a result, at 3 GeV the impedance threshold drops below machine impedance and thus the beam is vulnerable to LMWI. However, for PEPII, with its dipole configuration being different for LER and HER, the beam at 3.1 GeV can have a large energy spread and hence is free from this instability. This situation manifests one major challenge for the e-ring design, i. e., the ring optics should be versatile enough to provide sufficient Landau damping for a wide range of beam energies. This estimation indicates the necessity to apply suppression mechanisms against the microwave instability for the JLEIC e-ring at low energy. Examples of such mechanisms include use of an alternative dipole configuration at low energy, the split-dipole concept in the eRHIC design [8], or damping wigglers. For the ion ring, the machine impedance is expected to be much smaller than the threshold impedance, so the beam is safe from this instability. For the electron ring, detailed simulations are needed to study the bunch lengthening due to potential-well distortion below the LMWI threshold, as well as the turbulent bunch lengthening and increase of energy-spread beyond the instability threshold.

Table 2: Longitudinal Microwave Instability (LMWI)

	PEP-II (LER)	**JLEIC** e-Ring			**JLEIC** p-Ring
E [GeV]	3.1	3	5	10	100
$\left\|Z_{\parallel}/n\right\|^{\text{ring}}$ [Ω]	~0.1	≤0.1 (expectation)			0.1
$\left\|Z_{\parallel}/n\right\|^{\text{th}}$ [Ω]	0.145	0.027	0.125	1.16	22.5
LMWI	s	u	m	s	s

Transverse Mode-Coupling Instability (TMCI)

For TMCI, the approximate theoretical threshold for transverse impedance is

$$\left|Z_{\perp}\right|^{\text{th}} \approx FE\,\nu_s / e\langle\beta_{\perp}\rangle I_{\text{peak}},$$

with F the bunch form factor ($F \sim 2\pi$ for short bunches). In Table 3, we compare this theoretical threshold, evaluated using parameters in Table 1, with the estimated upper limit of machine transverse impedance $\left|Z_{\perp}\right|^{\text{ring}}$, obtained using impedance budgets of existing machines as references. The comparison shows that the beams are stable with regard to TMCI. Note that there are large uncertainties in both the machine traverse impedance and the simple back-of-envelope formula. Detailed studies of TMCI require an accurate JLEIC impedance model. Such

studies include solving the eigenvalue problem of the Vlasov equation [9] or macroparticle tracking that takes into account potential-well distortion in the longitudinal phase space and many other effects [10]. Additionally, special attention needs to be paid to the Christmas-tree-like equilibrium longitudinal charge distribution for the proton bunch under strong electron cooling, which has a very dense core with long tails [11]. Space-charge effects on TMCI will also be assessed, especially for the ion bunches during their formation process [12].

Table 3: Transverse Mode-Coupling Instability (TMCI)

	PEP-II (LER)	**JLEIC** e-Ring			**JLEIC** p-Ring
E [GeV]	3.1	3	5	10	100
$\lvert Z_\perp\rvert^{\text{ring}}$ [MΩ/m]	≤0.1	≤0.1 (expectation)			≤0.5
$\lvert Z_\perp\rvert^{\text{th}}$ [MΩ/m]	0.28	0.22	0.60	2.4	119
TMCI	s	s			s

Coupled-Bunch Instabilities

In the collider rings, narrowband impedances from RF cavities, crab cavities and various other mode-trapping components can cause longitudinal or transverse coupled bunch instabilities (LCBI or TCBI). The JLEIC electron ring plans to use the PEP-II RF cavities, with the RF HOM parameters listed in Ref. [13]. For the JLEIC ion ring, an RF cavity design was developed with waveguide couplers for efficient HOM damping. The corresponding HOM parameters are listed in Ref. [14]. With these RF HOMs, as well as the resistive wall impedance and broad-band impedance $\left(Z_\parallel^{BB}\right)_0 = 2\Omega$, we estimate the growth rate for the coupled-bunch instabilities (CBI) using ZAP [15] (with Sacherer-Zotter's formulas). For the selected set of collision energies for the electron and proton beams, results are shown in Tables 4 and 5. This calculation assumes an even bunch filling pattern, and Gaussian and parabolic bunch profiles for electron and ion beams respectively. In addition, a non-zero chromaticity of $\xi = 1$ and a finite betatron tune spread of 3e-04 are assumed for the TCBI calculations for both the electron and the proton beams.

In Table 4 and 5, $\tau_{a=1}^{\parallel}$ and $\tau_{a=2}^{\parallel}$ are the growth time for the longitudinal dipole and quadruple modes respectively, and $\tau_{a=0}^{\perp}$ and $\tau_{a=1}^{\perp}$ correspond to the growth time for the transverse rigid and dipole modes. Here $\tau_{\text{damp}}^{\parallel}$ (or $\tau_{\text{damp}}^{\perp}$) for the e-ring represents the natural longitudinal (or transverse) damping time due to synchrotron radiation, while $\tau_{\text{damp}}^{\parallel}$ and $\tau_{\text{damp}}^{\perp}$ for the p-ring are the damping times for the proton beam due to the strong electron cooling [16] in the JLEIC design. Note that for the electron ring, the lowest-energy beam (E_e =3 GeV) has the fastest growth time, i.e., $\tau_{a=1}^{\parallel}$=2.9 ms for LCBI and $\tau_{a=0}^{\perp}$ =1.6 ms for TCBI. With growth rates much faster than the natural damping rates in the low-energy regime, these instabilities are manageable by fast feedback systems (damping time < 1ms) as used in modern electron storage rings. For the proton beam, the resistive-wall induced quadruple mode has a fast LCBI growth time, $\tau_{a=1}^{\parallel}$ =6.2 ms. This is a result of the single-bunch mode spectra for parabolic proton bunch profile. It is well known that electron cooling will change the bunch profile significantly, and its effect on LCBI growth rate remains to be studied. Many topics of CBI and its mitigation schemes need to be addressed by careful studies, such as (1) effects of realistic uneven bunch pattern (with injection/ejection gaps and/or ion clearing gaps), (2) the joint effects of HOMs from both the accelerating/focusing RF cavities and the crab cavities, and (3) the Landau damping for transverse coupled-bunch instability due to tune-shift spread from beam-beam interaction.

Table 4: LCBI in JLEIC

	e-Ring			p-Ring
E [GeV]	3	5	10	100
$\tau_{a=1}^{\parallel}$ [ms]	2.9	4.1	72.8	30.7
$\tau_{a=2}^{\parallel}$ [ms]	31	43	466	6.2
$\tau_{\text{damp}}^{\parallel}$ [ms]	187	40.5	5.1	> 30 min

Table 5: TCBI in JLEIC

	e-Ring			p-Ring
E GeV]	3	5	10	100
$\tau_{a=0}^{\perp}$ [ms]	1.6	2.7	64	24.4
$\tau_{a=1}^{\perp}$ [ms]	12.8	19.6	39.8	805
$\tau_{\text{damp}}^{\perp}$ [ms]	375	81	10	> 30 min

Electron Cloud in the Ion Ring

In an ion ring, the ionization of residual gas and the beam-loss induced surface emission provide the source for the primary electrons, while the electron cloud build-up comes mainly from the secondary electron production [17]. The electron cloud build-up behaviour depends on how the ion beam structure is compared to the reflection time of secondary electrons. For different stages of ion bunch formation in JLEIC, the build-up of electron cloud and its impact on the ion bunch stability can behave very differently. When the bunches are long and the repetition rate is low, as in conventional ion rings, electrons generated ahead of the bunch centre are trapped by the beam potential and are released toward the tail of the bunch, the so called trailing-edge effect. In the collision scenario, the high repetition rate and short bunches of the ion beam

make the e-cloud effect similar to those encountered by positron beams in modern lepton colliders. In such case the electron cloud density rises up rapidly and saturates at the neutralization density. For the proton beam at E_p =100 GeV, the neutralization density is

$$\rho_{sat} = \frac{N_b}{\pi b^2 L_{sep}} = 2\times10^{12}\ \mathrm{m}^{-3}\ ,$$

as modelled in Ref. [18] for a similar set of parameters. The threshold for the electron-cloud induced single-bunch transverse mode-coupling instability (TMCI) is estimated using the two-particle model [19],

$$\rho_{th} = \frac{2\gamma Q_s}{\pi r_p C\langle\beta_y\rangle} = 1.7\times10^{13}\ \mathrm{m}^{-3}.$$

With $\rho_{sat} < \rho_{th}$, the bunch is stable from the electron-cloud induced strong head-tail instability. The electron cloud may also cause coupled-bunch instability for the JLEIC ion beam, which could be more concerning and requires detailed simulations.

Ion Effect in the Electron Ring

As the electron bunch trains circulate in a storage ring, they scatter with the residual gas molecules and produce ion particles. The ions could be trapped by the e-beam potential well and cause many undesirable effects for the electron beam, such as emittance growth, tune shift, halo formation, and coherent coupled-bunch instabilities. For a symmetric bunch pattern, and for constant rms bunch sizes, the critical mass for the ions to be trapped in either *x*-motion or *y*-motion is given by [20]

$$A_{x,y}^{trap} = \frac{r_p N_b L_{sep}}{2\sigma_{x,y}(\sigma_x+\sigma_y)}.$$

Our estimation shows that for the JLEIC ion ring all ion molecules ($A \geq 2$) will be trapped for even bunch fill.

The ions produced from ionization scattering and then trapped by the beam potential can be cleared by leaving gaps in between the bunch trains [21]. However, even with the ions being cleared after each turn by a clearing gap (or gaps), there is still the fast beam-ion instability (FBII) [22] that could develop within the bunch train during a single-turn circulation. Turn-by-turn, the transverse dipole motion for the electron bunches is propagated within a bunch train and gets amplified, with the dipole amplitude increasing in time and along the bunch train. Under the assumptions that (1) the force between the ion and electron beam is linear to their relative dipole offsets and (2) oscillation frequency is identical for all ions, the growth time τ_g for FBII is given by

$$y_b(t) \propto \left(t/\tau_g\right)^{-1/4} e^{\sqrt{t/\tau_g}},$$

$$\tau_g^{-1}[s^{-1}] = 5\,p[Torr]\frac{N_b^{3/2} n_b^2 r_e r_p^{1/2} L_{sep}^{1/2} c}{\gamma\sigma_y^{3/2}(\sigma_x+\sigma_y)^{3/2} A^{1/2}\omega_\beta}.$$

For realistic beams, the horizontal charge distribution could result in the spread of the ion oscillation frequency and therefore the Landau damping of FBII. The dipole amplitude growth in such case is characterized by the e-folding time [23, 24]

$$y_b \propto e^{t/\tau_e},\ \ \tau_e^{-1} \approx \tau_g^{-1}\frac{c}{4\sqrt{2\pi}L_{sep}n_b a_{bt} f_i}$$

for f_i the coherent ion oscillation frequency and a_{bt} the ion frequency variation. For a single bunch train in the JLEIC electron ring, τ_g and τ_e are shown in Table 6 (for a_{bt} =0.5). Here for E_e=10 GeV, the growth time is comparable to its counterpart for the PEPII HER beam. However, for E_e=3-5 GeV, the growth time is one or two orders of magnitude shorter and is consequently a serious concern for the electron beam stability. Further reduction of the growth rate is expected if the frequency spread of the ion beam, induced by the beam-size variation due to betatron oscillation, is taken into account. Possible mitigation methods include using (1) chromaticity to Landau damp the FBII, (2) clearing electrode, or (3) multiple bunch trains to reduce the growth amplitude. Comprehensive numerical modelling, for both FBII and the mitigation schemes, need to be performed for JLEIC. Further studies need to combine FBII with the beam-beam induced tune spread, along with the coupled-bunch beam-beam instability in the gear-change collision arrangements [25].

Table 6. Growth time of FBII for JLEIC e-Ring

E_e [GeV]	3	5	10
τ_c [μs]	0.01	0.11	13.9
τ_e [ms]	0.02	0.1	3.2

MCBI IN ERHIC

In eRHIC, a polarized electron beam (2.5 to 18 GeV) collides with a polarized proton beam (41 to 275 GeV) or beams of other ion species. This EIC design takes full advantages of the existing RHIC, by using one of the RHIC rings as the EIC hadron collider ring and adding two electron rings in the same tunnel: a 400 MeV to 18 GeV rapid cycling synchrotron (RCS) and a full-energy electron collider ring. A schematic layout of eRHIC is shown in Fig. 2.

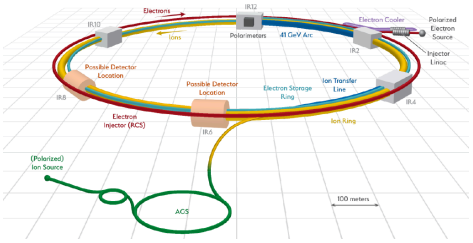

Figure 2: Schematic layout of eRHIC

The coherent instabilities in eRHIC are studied for the electron and hadron beams at several collision energies [26, 27]. The impedance-induced instabilities are modelled

by particle tracking using TRANFT [10]. In this code, the beam is represented by 5 bunches (with periodic conditions for even bunch fill) and up to 10^5 macroparticles per bunch. The particles experience interaction with both short-range and long-range wakefields, along with fields for certain mitigation mechanisms. For the electron beam in the collider ring, weak-strong beam-beam interaction from collision at IR is also included.

Collective Effects in the Electron Collider Ring

For this study, particle tracking is performed for electron beam at 5, 10 and 18 GeV. Here the broadband impedances consist of the geometric, resistive and coherent synchrotron radiation (CSR) impedances. The HOM of the RF cavity (residing near an absorber) and resistive wall impedance are respectively the major contributors for the longitudinal and transverse narrowband impedances. Tracking studies show that at the selected energies, the bunch charge at threshold of microwave instability is two or three times larger than its nominal value, and the increase of bunch length is insignificant. At 10 GeV, the longitudinal coupled-bunch instability can be mitigated by a longitudinal damper with $\mathrm{Im}(Q_s)$=0.001, and the transverse coupled-bunch instability can be Landau damped by beam-beam tune spread with the nominal beam-beam parameter of 0.075~0.1.

The fast ion instability is studied by another code [28]. In this model, 40 ion slices are distributed around the ring to account for the spread of the ion oscillation frequency, due to variation of the transverse bunch size caused by betatron motion. With Landau damping from beam-beam interaction, simulated by Bassetti-Erskine kick once per turn, the threshold for maximum density of CO gas (for nominal gas temperature and pressure) is found to be challenging but achievable.

Collective Effects in the Hadron Collider Ring

Beam dynamics is studied using TRANFT for proton beam at 22.8, 41, and 275 GeV. Because an existing RHIC ring will be used as the EIC hadron collider ring, the short-range wakefield can be constructed from the broadband impedance directly measured from RHIC, while the long-range wakefield can be constructed from the dominant HOMs from the RHIC RF cavity. Additionally, space charge and resistive wall effects are included in the particle tracking. The simulations show that at the microwave instability threshold, the bunch charges at different energies could be an order of magnitude higher than their nominal values, and the bunch lengthening is insignificant. The growth rates for the longitudinal and transverse coupled-bunch instability agree well with simplified analytical results. However, there is an increase of the transverse emittance at 22.8 GeV, probably due to the numerical handling of the space-charge force in the simulation.

Electron cloud is a serious concern for the EIC hadron ring, in terms of high cryogenic loss and beam instability. The plan is to coat the arc chambers with copper. Further reduction of the heat load at high current operation can be achieved by applying an additional layer of coating consisting of amorphous carbon.

CONCLUSIONS

In this paper, we presented the status of our preliminary study of coherent instabilities and mitigation in the two EIC designs, JLEIC and eRHIC. The discussions show that an EIC takes the collider design to a new parameter regime, where the hadron beam pattern is similar to those in lepton colliders whereas the design of the electron ring needs to ensure electron beam stability for a wide range of energies. These new regimes pose many challenges to the mitigation of coherent beam instabilities. Recently with BNL chosen to host the EIC, the EIC design enters a brand-new phase. Comprehensive studies of the impedance budget, behavior of coherent instabilities, and the possible interplays of different instability mechanisms and their mitigations are currently under way.

ACKNOWLEDGEMENT

We thank F. Marhauser, R. Rimmer, J. Guo, T. Michalski, K. Deitrick, A. Hutton, and M. Blaskiewicz for helpful discussions.

REFERENCES

[1] Ya. Derbenev *et al.,* "Achieving High Luminosity in an Electron-Ion Collider", proceedings of HB2010 Workshop (2010).
[2] Y. Zhang, "JLEIC Baseline Update and New Parameters", https://www.jlab.org/indico/event/210/ (2017).
[3] "PEP-II an Asymmetric B Factory", Conceptual Design Report, SLAC-418 (1993).
[4] D. Zhou, SuperKEKB mini optics meeting (2015).
[5] R. Li *et al.,* pg. 90, proceedings of eeFACT2018 (2018).
[6] S. Benson, Cool17 Workshop (2017).
[7] A. Hutton, private communication (2018).
[8] C. Montag, Proc. of IPAC 2017, pg 3035 (2017)
[9] Y.H. Chin, MOSES 2.0, CERN/LEP-TH/88-05 (1988).
[10] M. Blaskiewicz, "The TRANFT User's Manual version 1.0", private communication (2017).
[11] A. Sidorin *et al.,* THAP01, Proceedings of COOL 2007 (2007).
[12] A. Burov, Phys. Rev. ST Accel. Beams 12, 044202 (2009); Erratum Phys. Rev. ST Accel. Beams 12, 109901 (2009).
[13] R. Rimmer *et al.,* "PEP-II RF Cavity Revisited", CBP Tech Note 197, LCC-0032 (1999).
[14] F. Marhauser and R. Rimmer, "Progress on the Design of the JLEIC Ion Ring Cavities", JLAB-TN-18-041, 2018.
[15] M. Zisman, S. Chattopadhyay, J.J. Bisognano, "ZAP USER'S MANUAL" LBL-21270 (1986)
[16] H. Zhang, "Cooling Simulation Studies", https://www.jlab.org/indico/event/210/ (2017).

[17] K. Ohmi *et al.*, PRSTAB 5, 114402 (2002).
[18] S. Ahmed *et al.*, "Computational Modeling of Electron Cloud for MEIC", Proc. of IPAC12 (2012).
[19] K. Ohmi, F. Zimmermann, PRL 85, p. 3821 (2000).
[20] Y. Baconnier, G. Brianti, CERN/SPS/80-2 (1980).
[21] M. Q. Baron, NIMA 243, 278 (1986).
[22] T.O. Raubenheimer and F. Zimmermann, Phys. Rev. E, Vol. 52, 5487 (1995).
[23] G. Stupakov, T.Raubenheimer, and F. Zimmermann, PRE, Vol. 52, 5499 (1995).
[24] F. Zimmermann *et al.,* SLAC-PUB-7617 (1997).
[25] V. S. Morozov *et al.,* "Study of Beam Synchronization at JLEIC", arXiv: 1606.09117 (2016).
[26] M. Blaskiewicz, private communication (2019).
[27] Electron Ion Collider of Brookhaven National Laboratory, pre-Conceptual Design Report (2019).
[28] M. Blaskiewicz, "Beam-beam damping of the ion instability", Proc. of NaPAC 2019 (2019).